

Distribution Agreement

In presenting this thesis as a partial fulfillment of the requirements for a degree from Emory University, I hereby grant to Emory University and its agents the non-exclusive license to archive, make accessible, and display my thesis in whole or in part in all forms of media, now or hereafter now, including display on the World Wide Web. I understand that I may select some access restrictions as part of the online submission of this thesis. I retain all ownership rights to the copyright of the thesis. I also retain the right to use in future works (such as articles or books) all or part of this thesis.

Zahra Manji

April 14, 2015

Time-dependent determination of inflammatory mediators
in a 5xFAD mouse model of Alzheimer's disease

By

Zahra Manji

Thota Ganesh, PhD.
Adviser

Department of Pharmacology, Emory University School of Medicine
Program in Neuroscience and Behavioral Biology

Thota Ganesh, PhD.
Adviser

Raymond Dingledine, PhD.
Committee Member

Melvin Konner, PhD., MD.
Committee Member

Samuel Sober, PhD.
Committee Member

2015

Time-dependent determination of inflammatory mediators
in a 5xFAD mouse model of Alzheimer's disease

By

Zahra Manji

Thota Ganesh, PhD.
Adviser

An abstract of
a thesis submitted to the Faculty of Emory College of Arts and Sciences
of Emory University in partial fulfillment
of the requirements of the degree of
Bachelor of Sciences with Honors

Department of Pharmacology, Emory University School of Medicine
Program in Neuroscience and Behavioral Biology

2015

Abstract

Time-dependent determination of inflammatory mediators in a 5xFAD mouse model of Alzheimer's disease By Zahra Manji

The inflammatory process has been shown to play a significant role in the pathogenesis of AD (Rubio-Perez and Morillas-Ruiz, 2012). Inflammatory mediators related to AD include glial cells such as astrocytes and microglia in addition to cytokines and chemokines. In neurodegenerative diseases such as Alzheimer's, inflammatory changes can facilitate neuronal dysfunction and cell injury and may be a potential mechanism that exacerbates these effects over time (Zhang and Jiang, 2015).

The goal of the current experiment is to analyze inflammatory gene expression in a time-dependent manner using the 5x Familial Alzheimer's disease (FAD) mouse model. A key question of interest is whether or not COX-2 differs between 5xFAD and WT mice. COX-2 has been shown to increase in Braak stages 0 – II, yet decrease in Braak stages V and VI. Therefore, this study aims to determine the time of COX-2 induction, and whether this is concurrent with plaque development during the early stages of AD.

In this experiment, quantitative real-time polymerase chain reaction (qRT-PCR) was used to analyze the mRNA fold changes of male and female WT and 5xFAD mice at 3 different time-points: 2-, 3-, and 4-months of age. The 9 genes that were examined were: COX-2, TNF- α , IL-1 β , CCL2, CXCL10, IL-6, GFAP, IBA1, and EP2. It was found that in 5xFAD males, COX-2 was continuously increasing from 2- to 4-months and was the only gene that was induced at 4-months. In 5xFAD females, both CXCL10 and GFAP were increasing from 2- to 4-months and were significantly upregulated at both 3- and 4-months. Essentially, this study can be used to better understand changes in inflammatory gene expression during the initial stages of AD where A β plaque pathology begins and continues to escalate over time.

Time-dependent determination of inflammatory mediators
in a 5xFAD mouse model of Alzheimer's disease

By

Zahra Manji

Thota Ganesh, PhD.

Adviser

A thesis submitted to the Faculty of Emory College of Arts and Sciences
of Emory University in partial fulfillment
of the requirements of the degree of
Bachelor of Sciences with Honors

Department of Pharmacology, Emory University School of Medicine
Program in Neuroscience and Behavioral Biology

2015

Acknowledgements

I would like to thank Dr. Asheebo Rojas, Dr. Thota Ganesh, Nadia Lelutiu, Dr. Nicholas Varvel, and Theon O'Neil for aid and guidance throughout the course of this project. I would also like to thank Dr. Melvin Konner and Dr. Samuel Sober for serving on my Honors Thesis Committee. Lastly, I would like to thank Dr. Raymond Dingleline for also serving on my Committee and for giving me the opportunity to perform my senior Honors Thesis in his lab.

Table of Contents

1. Introduction.....	2
2. Materials and Methods.....	13
3. Results.....	19
4. Figures and Tables	
a. Figure 1a: % Weight vs. Time of 4-month WT and 5xFAD males.....	19
b. Figure 1b: % Weight vs. Time of 4-month WT and 5xFAD females.....	19
c. Figure 2: mRNA fold changes for 2-, 3-, and 4-month 5xFAD males and females for all genes of interest.....	22
d. Figure 3: mRNA fold change for 4-month WT and 5xFAD females for CXCL10 and GFAP.....	23
e. Figure 4: mRNA fold change for 4-month WT and 5xFAD males and females for COX-2.....	23
f. Figure 5: Congo red staining using IBA1 primary antibody spanning the cortex in a 4-month WT and a 4-month 5xFAD female mouse.....	24
5. Discussion.....	25
6. Future Directions.....	29
7. Conclusion.....	31
8. Limitations.....	32
9. References.....	33
10. Supplementary Material	
a. Figure 6: Human FAD mutations present on APP and PSEN1 in the 5xFAD mouse model.....	40
b. Figure 7: COX-2 Signaling Cascade (Jiang and Dingledine, 2013).....	41
c. Figure 8: Generation of A β from APP.....	41
d. Table 1a: Mean $\Delta\Delta$ CT values with standard deviations for 2-month WT and 5xFAD males and females.....	42
e. Table 1b: Mean mRNA fold changes with 95% Confidence Interval for 2-month WT and 5xFAD males and females.....	42

f.	Table 2a: Mean $\Delta\Delta\text{CT}$ values with standard deviations for 3-month WT and 5xFAD males and females.....	43
g.	Table 2b: Mean mRNA fold changes with 95% Confidence Interval for 3-month WT and 5xFAD males and females.....	43
h.	Table 3a: Mean $\Delta\Delta\text{CT}$ values with standard deviations for 4-month WT and 5xFAD males and females.....	44
i.	Table 3b: Mean mRNA fold changes with 95% Confidence Interval for 4-month WT and 5xFAD males and females.....	44
j.	Table 4a: <i>P</i> -values using ΔCT values of 2-, 3-, and 4-month males.....	45
k.	Table 4b: <i>P</i> -values using ΔCT values of 2-, 3-, and 4-month females.....	45
l.	Table 5: Mean CT values for housekeeping gene, GAPDH, for 2-, 3-, and 4-month WT and 5xFAD males and females.....	46
m.	Table 6: Table of primers used for qRT-PCR.....	46
n.	Table 7: Sample sizes for all 2-, 3-, and 4-month male and female WT and 5xFAD mice.....	46

Time-dependent determination of inflammatory mediators in a 5xFAD mouse model of Alzheimer's disease

Zahra Manji

Emory University School of Medicine, Department of Pharmacology, Atlanta, GA 30322, U.S.A.

Key Words

Alzheimer's disease, inflammation, gliosis, pro-inflammatory cytokines, chemokines, cyclooxygenase-2, prostaglandins, EP2

Abbreviations

Alzheimer's disease (AD), familial Alzheimer's disease (FAD), beta-amyloid (A β), amyloid-precursor protein (APP), presenilin 1 and 2 (PSEN1 and PSEN2), central nervous system (CNS), cerebrospinal fluid (CSF), β -secretase 1 (BACE1), quantitative real-time polymerase chain reaction (qRT-PCR), tumor necrosis factor- α (TNF- α), interleukin-1 β (IL-1 β), interleukin-6 (IL-6), chemokine (C-C motif) ligand 2 (CCL2), chemokine (C-X-C motif) ligand 10 (CXCL10), cyclooxygenase-1 and 2 (COX-1 and COX-2), glial fibrillary acidic protein (GFAP), ionized calcium-adapter molecule 1 (IBA1), glyceraldehyde 3-phosphate dehydrogenase (GAPDH)

Introduction

Alzheimer's disease Background

Alzheimer's disease (AD) is the most common neurodegenerative disorder to date, which progressively destroys an individual's memory, ability to learn, reason, communicate, and execute daily activities (Rubio-Perez & Morillas-Ruiz, 2012). The disease is divided into either familial or sporadic cases. Familial AD mainly occurs due to mutations in the genes for amyloid precursor protein (APP), presenilin 1 (PSEN1), and presenilin 2 (PSEN2) (Piaceri, Nacmias, and Sorbi, 2013). Sporadic AD may be attributable to genetic and environmental factors, yet its underlying etiology is still unknown (Piaceri, Nacmias, and Sorbi, 2013). The most common form of AD is late-onset, affecting those that are 65 years of age and older, while early-onset AD occurs between the ages of 30 to 65. Familial AD, which only accounts for 5% of all AD cases, has predominantly been linked with early-onset cases yet late-onset cases have also been described (Bekris et al., 2010). Interestingly, patients can present with preclinical signs where they have yet to express AD pathology and have not been given a definitive diagnosis of the disease. Identifying potential biomarkers could be highly effective in the preclinical stages of AD where physicians can identify and track changes in the disease prior to significant cognitive impairment (Sperling et al., 2010). Therefore, there lies a need to elucidate a possible link between the pathophysiological process and the emergence of clinical symptoms in order to develop treatment to modify and delay cognitive decline evidenced in AD.

AD Pathology

The major hallmarks of AD are extracellular beta-amyloid (A β) neuritic plaques and intracellular neurofibrillary tangles (Rubio-Perez & Morillas-Ruiz, 2012). A β plaques are generated through the proteolysis of APP, which is a membrane-spanning protein with a large extracellular and a small intracellular domain (Turner et al., 2003). The enzyme that first cleaves APP extracellularly is known as β -secretase 1 (BACE1). This leaves behind a soluble fragment that later gets degraded as well as another fragment known as C99 that remains bound to the cell membrane. A second enzyme, γ -secretase, cleaves C99, releasing the intracellular domain of APP and generating A β (Figure 8). This reaction is regulated by PSEN1, which is essential for γ -secretase activity. As plaques continue to form, they essentially block cell-to-cell signaling at synapses and become highly toxic to nerve cells.

Neurofibrillary tangles are composed of the protein tau. In healthy neurons, tau is an important component of microtubules to help transport nutrients and mitochondria from the cell bodies to the ends of the axons and vice versa. However, in AD, tau becomes hyperphosphorylated, causing it to bind together and form tangled threads (Braak, Braak, and Strothjohann, 1994). Hyperphosphorylation also causes pieces of soluble tau to accumulate, leading to further cognitive impairment (LaFerla, 2008). Plaques and tangles together promote the loss of nerve cell connections. As a result of neuronal death, the brain atrophies over time, leading to the loss of memory and mental functioning. Ultimately, the disease attacks nerve cells in all parts of the cortex and surrounding tissue from which there is no cure or recovery.

Inflammation has also been implicated in the pathogenesis of AD. This process involves various cellular and molecular changes such as the recruitment of peripheral immune cells, induction of intracellular signaling pathways, and release of inflammatory mediators in the brain (Zhang and Jiang, 2015). These changes can either alone or in combination facilitate the neuronal dysfunction and death associated with AD (Zhang and Jiang, 2015). Interestingly, A β accrual can also lead to an increase in inflammation. This vicious cycle suggests that inflammation may be a trigger or a consequence associated with the pathological changes of AD.

Inflammation Background

Inflammation is the immune system's response to a particular injury. It is not only involved in neurological diseases such as Alzheimer's, but also in other conditions such as arthritis, cancer, stroke, and cardiovascular disease (Ricciotti and FitzGerald, 2011). Inflammation is the body's ability to self-protect itself, and it aims to remove harmful stimuli such as damaged cells and pathogens in order to initiate the healing process. Analogously, neuroinflammation is when the brain activates the innate immune system to protect the central nervous system (CNS) from infection or disease (Zhang and Jiang, 2015). There are two classifications of inflammation: acute and chronic. The acute phase is the initial response of inflammation. It involves a rapid influx of blood granulocytes, mainly neutrophils, followed by monocytes that mature into macrophages and proliferate to target the injured tissue (Ricciotti and FitzGerald, 2011). Acute inflammation aims to remove necrotic tissue and initiate repair. Prolonged inflammation is also known as chronic inflammation. It is principally due to the inability of proper tissue restoration (Rubio-Perez & Morillas-Ruiz, 2012). Chronic inflammation can lead

to scarring, excessive tissue damage, and loss of organ function (Ricciotti and FitzGerald, 2011). This indicates that inflammation not only acts as a defensive response, but it can also be a potentially threatening process.

Gliosis

The two main types of glial cells of the CNS are astrocytes and microglia. In AD, glial cells can either proliferate or hypertrophy in response to CNS damage.

Unfortunately, the blood brain barrier prevents leukocytes to enter the CNS from the periphery. Due to this, activating specific immune cells known as microglia is a different approach to tackle the site of injury (Zhang and Jiang, 2015). Microglia account for 5% – 10% of the adult brain cell population (Zhang and Jiang, 2015). They act as macrophages and are present in all stages of brain development. Moreover, microglia are highly sensitive, and therefore, they are able to respond to the slightest alterations in the cellular environment. Their main functions include facilitating host defense by destroying pathogens, eliminating deleterious debris, promoting tissue repair, as well as regulating homeostasis (Glass et al., 2010).

Microglia are also associated with the neuronal death and cognitive decline evidenced in AD. For example, in a triple transgenic model of AD (3 x Tg-AD), Rodriguez et al. (2010) discovered a significant increase in activated microglia at 12 (by 111%) and 18 (by 88%) months of age compared to non-transgenic (non-Tg) controls. Additionally, they found that the activation of microglia was associated with A β plaque formation and smaller A β deposits. Microglia also try to limit the growth of early senile plaques and minimize inflammatory changes in the brain (Scheffler et al., 2011). Moreover, microglia secrete proteolytic enzymes such as the insulin-degrading enzyme,

matrix metalloproteinase, and plasminogen-plasmin complex, which degrade A β (Leissring et al., 2003; Li et al., 2011). Microglia can also secrete soluble factors simultaneously such as glia-derived neurotrophic factor in order to facilitate the survival of neurons (Liu and Hong, 2003). While there is a vast amount of evidence to support the role of microglia in neuroprotection and A β clearance, it is still unknown why A β continuously accumulates and why AD pathology progressively worsens with age (Zhang and Jiang, 2015).

Along with microglia, astrocytes are the second class of glial cells in the CNS. They account for 35% of the total cell population in the CNS (Zhang and Jiang, 2015). One of the main functions of astrocytes is to create an optimal environment for proper neuronal functioning. For instance, they remove debris and toxins from cerebrospinal fluid (CSF), regulate neurotransmitters, produce trophic factors, and maintain ion concentrations and redox potentials. Astrocytes may also provide trophic support to neurons and form a protective barrier between neurons and A β deposits, leading to A β clearance and degradation (Roßner et al., 2005). However, once astrocytes become injured and are unable to execute their functions, they can promote or even intensify neuronal dysfunction (Sidoryk-Wegrzynowicz et al., 2011). Reactive astrocytes are also able to express BACE1, which may lead to A β accumulation as seen in an aged transgenic mouse model (Hartlage-Rübsamen et al., 2003; Roßner et al., 2005). Therefore, as astrocytes encompass the largest percentage of CNS brain cells, they could be an essential source of A β accumulation as a result of AD neuroinflammation (Zhao et al., 2011). Once microglia and astrocytes are activated, they release numerous inflammatory mediators such as cytokines and potentially cytotoxic

substances such as chemokines, arachidonic acid derivatives, and prostanoids (Heneka and O'Banion, 2007). In essence, not only can glial cells assist in neuroprotection, but they have also been closely associated with the pathological features of AD.

Pro-inflammatory Cytokines and Chemokines

Cytokines are small, nonstructural proteins secreted from various cell types. They can induce chronic neuroinflammation, which has been seen as one of the major mechanisms associated with AD pathology (Zhang and Jiang, 2015). A key cytokine involved in neurological diseases is tumor necrosis factor- α (TNF- α). TNF- α regulates processes such as apoptosis, or cell death, differentiation, and inflammation (Zhang and Jiang, 2015). In a mouse model of AD, it has been shown that TNF- α regulates APP and induces A β production mainly by increasing the expression of BACE1 and the activity of γ -secretase (Liao et al., 2004). In relation to human studies, Gezen-Ak et al. (2013) demonstrated that compared to age-matched healthy controls, patients with early onset (< 65 years of age) as well as late onset (> 65 years of age) AD have significantly greater serum TNF- α levels. However, other studies have not determined a clear correlation with TNF- α and A β -42 levels, which is one of the major components of senile plaque deposition. Therefore, further research needs to be performed to better discern the roles of TNF- α in AD inflammation.

Interleukin-1 β (IL-1 β) is another cytokine involved in the inflammatory response whose functions include cellular proliferation, differentiation, and apoptosis. It is produced by activated macrophages and plays a role in the pathogenesis of AD. Previous studies have illustrated that IL-1 β promotes A β production by stimulating γ -secretase activity in neurons (Liao et al., 2004). Moreover, Rogers et al. (1999) showed

that enhanced translation of IL-1 β increased APP synthesis in astrocytes. Other studies have revealed that sustained IL-1 β expression induced tau protein phosphorylation, possibly intensifying tau pathology in a mouse model of AD (Ghosh et al., 2013). Interestingly, one study showed that prolonged IL-1 β expression did not lead to overt apoptosis in the hippocampus of an APP^{swe}/PS1^{dE9} mouse model (Matousek et al., 2012). While IL-1 β can facilitate AD pathologies, its underlying molecular mechanism in this disease needs to be further understood based on differing results of past studies.

Interleukin-6 (IL-6) is a chief cytokine of the CNS. It is secreted by T-cells and macrophages in order to initiate the inflammatory response after injury or disease. In the AD brain, IL-6 promotes the recruitment of microglia and astrocytes to release additional pro-inflammatory cytokines (Querfurth and LaFerla, 2010). IL-6 can also stimulate tau phosphorylation in neurons, paralleling with one of the functions of IL-1 β (Qi et al., 2012). Past studies have suggested that IL-6 polymorphisms could be an increased risk factor in AD (Chen et al., 2012; Qi et al., 2012). This is important to consider since Alzheimer's is a chronic condition, and genetic, epigenetic, and environmental factors all play important etiological roles in the disease.

Along with pro-inflammatory cytokines, chemokines, which are a large family of proteins controlling leukocyte movement, also play an important role in acute and chronic inflammation (Viola and Luster, 2008). There are two types of chemokines: α chemokines and β chemokines. The α chemokines have an amino acid that separates the first two cysteine residues of the mature protein (CXC) while the β chemokines have adjacent cysteine residues (CC) (Viola and Luster, 2008). Chemokine (C-C motif) ligand 2 (CCL2) was one of the first chemokines to be identified and is a powerful

monocyte attractant. Moreover, CCL2 and its receptor, CCR2, are able to recruit mononuclear phagocytes in order to engulf infectious agents during the inflammatory response (El Khoury and Luster, 2008). Not only is CCL2 expressed in reactive microglia in senile plaques, but it is also induced by A β in microglia and facilitates microglia chemotaxis (Ishizuka et al., 1997). Another study found that in an APP Tg2576/CCR2-null mouse model, CCR2 deficiency significantly reduced the number of microglia before the formation of plaques (El Khoury et al., 2007). These studies suggest that CCL2-CCR2 interactions may migrate microglia to sites of A β deposition, and early microglia accumulation could be neuroprotective in AD.

Another chemokine that has a critical role in controlling the entry of leukocyte subsets into the brain is (C-X-C motif) ligand 10 (CXCL10) (Michlmayr and McKimmie, 2014). It is expressed by nerve, glial, and stromal cells in a variety of CNS diseases (Michlmayr and McKimmie, 2014). The receptor for CXCL10 is CXCR3, which is expressed on neurons in AD. Interestingly, knockout of this receptor in an APP/PSEN1 transgenic mouse model of AD has been shown to reduce A β plaque burden and rescue memory impairment, indicating that CXCR3 signaling may mediate AD-like pathology (Krauthausen et al., 2015). Additionally, when CXCL10 binds to its receptor, it has been suggested that this could trigger extracellular signaling pathways, regulating kinase activity and ultimately leading to neuronal death and apoptosis (Sui et al., 2006; Cho et al., 2009; Nelson and Gruol, 2004). Essentially, this may be one possible mechanism for memory loss evidenced in AD.

Prostaglandins, Cyclooxygenase, and EP2

In addition to these several proteins, glial cells release lipid molecules that are also involved in the inflammatory response of neurological disorders. For instance, prostaglandins are enzymatically derived from arachidonic acid, a polyunsaturated omega-6 fatty acid. Prostaglandins can cause vasodilation, fever, pain, and are found in most tissues and organs. However, once a tissue becomes inflamed, the biosynthesis of prostaglandins increases significantly (Ricciotti and FitzGerald, 2011). Prostaglandins are unique because unlike the majority of hormones, they are not secreted from a gland. Instead, they are produced by a chemical reaction in the infected area by the enzyme cyclooxygenase (COX). There are two types of COX enzymes. COX-1 is responsible for maintaining baseline levels of prostaglandins and contributes to homeostasis (Ricciotti and FitzGerald, 2011). Conversely, COX-2 is induced by inflammatory stimuli, hormones, and growth factors (Ricciotti and FitzGerald, 2011). COX-2 acts as the chief source of prostanoid formation in proliferative diseases such as cancer. It also contributes to inflammation of the CNS, which is a key feature in the pathophysiology of neurodegenerative diseases such as Alzheimer's.

There are 4 types of bioactive prostaglandins: prostaglandin (PG) E₂ (PGE₂), prostacyclin (PGI₂), prostaglandin D₂ (PGD₂), and prostaglandin F_{2α} (PGF_{2α}). PGE₂ plays a critical role in neuroinflammation and modulates the expression of various inflammatory mediators by microglial cells (Jiang et al., 2013; Ricciotti and FitzGerald, 2011). PGE₂ exerts its effects by acting on four different types of receptors: EP1, EP2, EP3, and EP4. The EP2 receptor is a G-protein coupled receptor mainly found in the brain, kidneys, and platelets. EP2 receptors couple to G_{αs} receptors that activate cyclic

AMP (cAMP), increasing intracellular concentrations of protein kinase A (PKA) to phosphorylate other downstream targets. Also, prostanoid receptors give rise to Ca^{2+} via the EP3 receptor. These changes can further contribute to inflammation, injury, and pain (Jiang and Dingledine, 2013). In relation to AD, Montine et al. (1999) showed that patients with probable AD had higher CSF concentrations of PGE_2 than age-matched controls. Liang et al. (2005) conducted a study to highlight the pro-inflammatory and pro-amyloidogenic functions of the EP2 receptor using the APPSwePS1 Δ E9 mouse model, which expresses an increase in the ratio of $\text{A}\beta_{42}$ to $\text{A}\beta_{40}$. It was found that deletion of the EP2 receptor showed a striking decrease in lipid peroxidation and was significantly associated with decreased levels of both $\text{A}\beta_{42}$ and $\text{A}\beta_{40}$ (Liang et al., 2015). Also, it has been demonstrated that PGE_2 increases APP gene expression *in vitro*, which has been associated with EP2 receptor activation in microglia (Lee, Knapp, and Wurtman, 1999; Pooler et al., 2004).

Rationale

This experiment aims to better understand the progression of inflammation in AD over time using a 5xFAD mouse model. This transgenic model expresses mutant human APP(695) with the Swedish (K670N/M671L), Florida (I716V), and London (V717I) mutations along with two human FAD mutations on PSEN1 (M146L and L286V) (Oakley et al., 2006). The APP mutations are located on chromosome 21 whereas the PSEN1 mutations are located on chromosome 14. The function of the Swedish double mutation on APP is to increase the activity of β -secretase 1, leading to cleavage of APP to generate more $\text{A}\beta$ peptides, which eventually cluster and form greater amounts of extracellular plaques. The PSEN1 mutations regulate the activity of γ -secretase,

leading to an increase in the levels of A β -42 to cause FAD (Takasugi et al., 2013). This model was chosen because it recapitulates A β plaque pathology as early as 2-months. Other transgenic mouse models such as Tg2576 that house the APP(695) Swedish mutation do not show plaques until 11 – 13 months of age.

The inflammatory mediators examined in this study were selected based upon their upregulation in the CSF of human AD patients. For instance, Brosseron et al. (2014) showed that IL-1 β , TNF- α , IL-6, and CXCL10 were all elevated in these patients whereas those with mild cognitive impairment (MCI) only showed an upregulation of IL-1 β and TNF- α . Other key genes of interest were GFAP and IBA1, which were selected to determine any change in astrocyte or microglia expression between 5xFAD mice and WT counterparts. Additionally, COX-2 and EP2 were selected as these genes have been implicated in neuroinflammation. During Braak stages 0 – II, COX-2 is highly upregulated, yet its expression decreases during Braak stages V and VI. Therefore, this study aims to determine the time at which COX-2 is upregulated, and whether its induction parallels with A β plaque deposition during the early stages of AD.

This experiment can be used as a control to better understand inflammatory mediator gene expression over time before modulating prostanoid receptors with an EP2 receptor antagonist. As COX-2 inhibitors have not been highly successful at alleviating the neurodegenerative effects associated with AD, placing a greater focus on more specific downstream targets such as the EP2 receptor can be beneficial for further experiments. Understanding how inflammatory gene expression changes over time may provide insight as to when is the appropriate time to administer treatment in future studies to potentially mitigate the neuroinflammation associated with AD.

Hypothesis

The hypothesis of this experiment is that the expression of critical inflammatory genes will increase in the 5xFAD mice compared to wild type mice over time.

A further question of interest is whether or not COX-2 differs between 5xFAD and WT counterparts. If so, what is its time-dependence, and is its expression correlated with A β plaque deposition?

Materials and Methods

Animals

All experiments and procedures were approved by the Institutional Animal Care and Use Committee at Emory University and were performed according to its guidelines. Male and female Charles River (C57BL/6) mice were purchased from Charles Rivers Laboratories. The 5xFAD mice were bred at Emory University's Division of Animal Resources. Mice were housed on a 12-hour light/dark cycle and were fed food and water *ad libitum*.

Experimental Design

This study examined inflammatory gene expression at 3 time-points: 2-, 3-, and 4-months. Each time-point had 4 groups: 5xFAD males and WT males, 5xFAD females and WT females. The mice were weighed one month after their time of birth and were continuously weighed each subsequent week. Once all mice grew for their respective lengths, they were sacrificed. A half-brain was frozen at -80°C and was then used to make cDNA and detect mRNA levels of inflammatory cytokines, chemokines, glial cells, COX-2, and EP2. The other half was fixed in paraformaldehyde (PFA) for 24 hours and

then placed in 30% sucrose in phosphate-buffered saline (PBS) for an additional 24 hours. Once the half-brain had sunk, it was transferred to 100% PBS and stored at 4°C.

Modified Irwin Test

The Irwin test, which is considered a functional operating battery, was used to check for overall health, locomotion, such as walking and running, hind limb movement, lacrimation, and vocalization. If the mice were walking and running normally, their hind limbs were moving, and they did not experience lacrimation or squealing upon being lifted, they received a score of 0. If the mice stayed in one place upon being touched but all other parameters were normal, they received a score of 2. If the mice were not walking or running and stayed in one place upon being touched without signs of any other problems, they received a score of 3.

RNA Extraction

Frozen brains were obtained from -80°C, and 1 mL of Trizol was added to the brain tissue. The homogenizer tip was washed with RNase Zap (Invitrogen) and 70% ethanol between each subsequent sample. The tissue was then homogenized for 30 seconds on ice. 200 µL of 99+% chloroform (Sigma) were added to the homogenized tissue. Each tube was shaken vigorously by hand for 15 seconds and incubated for 2 – 3 minutes at room temperature. The samples were centrifuged at 12,000x g for 15 minutes at 4°C. 150 µL of the upper phase were transferred to a new RNase-free tube, and 150 µL of 70% ethanol were added. The samples were loaded onto a spin cartridge and centrifuged for 1 min at 12,000x g (Sorvall). Using the PureLink RNA Mini Kit (Ambion, Invitrogen), the samples were washed with 350 µL of Wash Buffer 1 and were spun for 1 minute at 12,000x g. Then, 10µL of DNase + 70 µL of RDD buffer were

added to each cartridge (Qiagen). The samples were left for 15 minutes at room temperature. The samples were washed again with 350 μL of Wash Buffer 1 and spun for 1 minute at 12,000x g. All samples then received 500 μL of Wash Buffer 2, and they were re-spun at 12,000x g for 1 minute. This step was repeated after which the samples were centrifuged for 1 minute at 12,000x g to dry the membrane with the attached RNA. Spin cartridges were transferred to a new RNase-free tube. Then, 30 μL of RNase-free water were added to each sample. The samples were left at room temperature for 5 minutes and were lastly centrifuged at 12,000x g for 5 minutes. RNA samples were frozen and stored at -80°C .

RNA Concentration

The RNA Concentration was measured using an Epoch Microplate Spectrophotometer (BioTek). 2 μL of each sample were used for RNA concentration, which were reported in $\text{ng}/\mu\text{L}$.

cDNA Synthesis

The total reaction volume for each sample, including RNA, RNase sterile water, and qScript cDNA SuperMix, was 20 μL . The volume of RNA (based on 1 μg) that was added varied for each sample, depending on its concentration. The volume of RNA in addition to 4 μL of qScript cDNA SuperMix (5X Concentrated) (Quanta BioSciences) was subtracted from 20 μL , and this difference was the volume of RNase sterile water that was added for each sample. The reagents were combined in 0.2-mL micro-tubes. They were then vortexed gently and briefly centrifuged to collect all components at the bottom of the reaction tube. Cycling conditions included: incubation for 5 minutes at 25°C , 30 minutes at 42°C , 5 minutes at 85°C , and held at 4°C . After the cDNA was

synthesized, it was diluted 25X (96 μ L of RNase sterile water for every 4 μ L of cDNA). The samples were stored at -20°C .

Quantitative Real-Time Polymerase Chain Reaction (qRT-PCR)

The reaction mixture per sample included 10 μ L of iQ SYBR Green Supermix (Quanta BioSciences), 0.8 μ L of a forward and reverse primer mix of 10 μ M, 1.2 μ L of RNase sterile water, and 8 μ L of cDNA. Duplicates were made for each sample, and the final volume for each sample was 20 μ L in the iQ5 Multicolor Real-Time PCR Detection Machine (Bio-Rad Laboratories). Cycling conditions included: 95°C for 2 minutes followed by 40 cycles of 95°C for 15 seconds and then 60°C for 1 minute. Melting-curve analysis was used to verify the single species PCR product. Fluorescent data were obtained at the 60°C step.

Data were analyzed using the comparative cycle threshold (CT) method for all genes of interest. Relative mRNA expression levels were then determined according to the $\Delta\Delta\text{CT}$ method. The mRNA fold changes were calculated by $2^{-\Delta\Delta\text{CT}}$ where $\Delta\Delta\text{CT} = \Delta\text{CT}$ for the gene of interest (5xFAD) – ΔCT reference (WT) (Landel et al., 2014). The $\Delta\text{CT} =$ the mean CT value for each gene of interest – the mean CT value for the housekeeping gene: glyceraldehyde 3-phosphate dehydrogenase (GAPDH), which was the control for quantification (Jiang et al., 2013).

Immunohistochemistry using Free Floating Sections

To visualize beta-amyloid plaque pathology, a 4-month old female WT and a 4-month old female 5xFAD mouse was used. 40-micron-thick sections were cut using a freezing microtome. Sections were washed 3 times for 10 minutes each in PBS. Endogenous peroxidase was quenched using 0.3% H_2O_2 (10 μ L + 1 mL PBS/well). The

samples were incubated for 30 minutes at room temperature. They were washed 3 times again for 10 minutes each in PBS. To block unspecific bindings, 0.3% Triton (100 μ L) + 50 μ L Goat-serum + 850 μ L PBS/well were added. The samples were incubated for 30 minutes at room temperature. Sections were then placed in 880 μ L PBS + 300 μ L Triton + 60 μ L Goat-serum + 6 μ L of IBA1 primary antibody per well. The sections incubated at 4°C overnight. The following day, sections were washed 3 times for 10 minutes in PBS. They were placed in 1 mL of PBS + 10 μ L Goat-serum + 2.5 μ L anti-goat secondary antibody per well. The sections were incubated at room temperature for 45 minutes and were then washed 3 times for 10 minutes each in PBS. Sections were placed in a well containing 1 mL PBS + 8 μ L Avidin + 8 μ L of Biotin. They incubated at RT for 45 minutes. The sections were again washed 3 times for 10 minutes each with PBS. They were placed in 5 mL of 0.1M PBS + 3 drops of SG Blue + 3 drops of H₂O₂ per 5 wells. Sections were washed 3 times for 10 minutes each in PBS. Sections were mounted on coated slides (Super Frost) and were left to dry for 2 hours at room temperature.

Congo Red Staining

Congo red is a histochemical stain, which is useful to detect amyloid deposition. It is also the gold standard dye that is used as a diagnostic tool for amyloidosis (Linke, 2006). Congo red staining is a method that stains amyloid protein aggregates when they are in a compact form rather than when they are in a diffuse form (Wilcock et al., 2006). It essentially binds to congophilic A β and conforms to the shape of plaques to illustrate AD pathology in tissue sections.

After sections were mounted on slides and finished drying, they were rinsed in water and placed in a pre-incubation solution (80% ethanol + 15 g NaCl/1 mL NaOH) for 20 minutes. Slides were then placed in Congo red staining solution (80% ethanol + 15 g NaCl/1 mL of NaOH + 5 g Congo red, which dissolved overnight) for 20 – 30 minutes. Slides were differentiated twice in 80% ethanol. They were then dehydrated in 96% ethanol for 1 min, 2 x in 100% ethanol for 2 minutes and 2 x Xylene for 5 minutes each. A coverslip with Pertex (Mounting Medium) was placed on the slides, which were then left to dry until images were taken using an Axio Observer A1 microscope.

Data Analysis

Data in Tables 1a, 2a, and 3a are presented as mean $\Delta\Delta\text{CT}$ value with standard deviation (SD). Data in Tables 1b, 2b, and 3b are presented as mean mRNA fold change with a 95% Confidence Interval (CI) for a normal distribution.

Statistical analyses were performed using GraphPad Prism Software. Analysis between 4-month male and female WT and 5xFAD weekly weights was performed using a 2-way ANOVA. Additionally, a 2-way ANOVA comparing the ΔCT values was used to determine whether the mRNA fold changes were significantly different between 5xFAD and WT counterparts. A Bonferroni post-hoc test was used on all 2-way ANOVA analyses to correct for multiple comparisons. $P < 0.05$ was considered to be statistically significant.

The statistical tests that compared 5xFAD mice to their WT counterparts were performed separately at each time-point. Analysis of males and females was also conducted separately as it has been shown that 5xFAD females express the pathology slightly sooner than 5xFAD males (Oakley et al., 2006).

Results

Weekly Weights and Modified Irwin Test

Weekly weights and modified Irwin test scores were taken to examine the overall health and functionality of the mice throughout the span of their growth periods. No difference was seen in the weights (as a %) and modified Irwin test scores for 4-month male WT (n = 3) and 5xFAD (n = 4) and 4-month female WT (n = 3) and 5xFAD mice (n = 4) ($P > 0.05$; 2-way ANOVA; Bonferroni post-hoc test; Figures 1a and 1b).

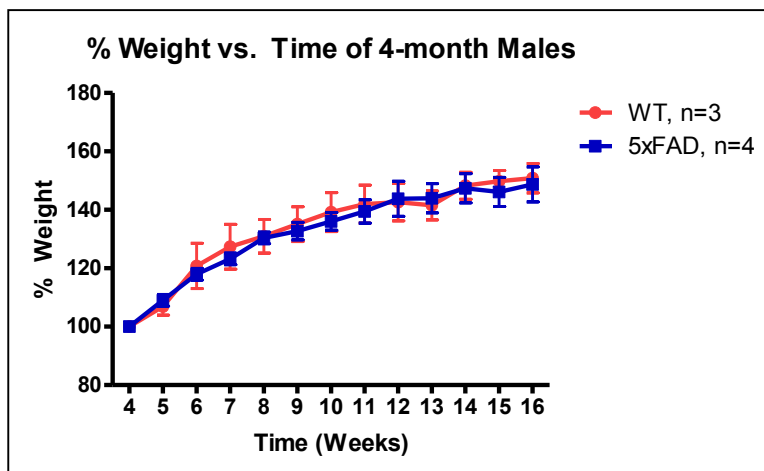


Figure 1a. % Weight vs. Time for 4-month WT (n = 3) and 5xFAD males (n = 4).

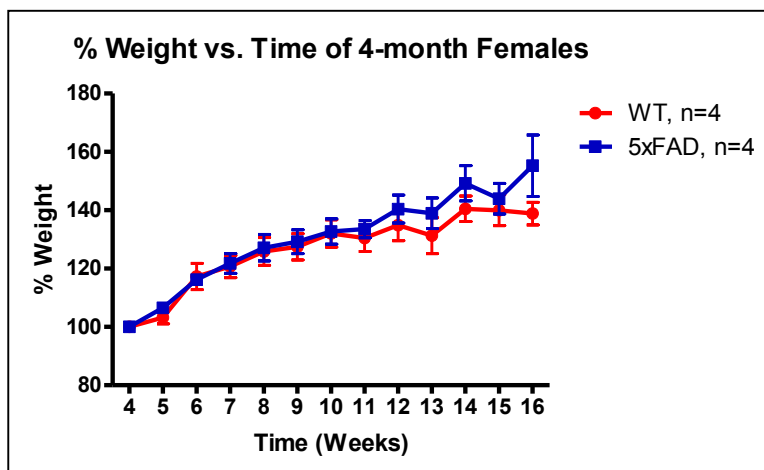


Figure 1b. % Weight vs. Time for 4-month WT (n = 4) and 5xFAD females (n = 4).

Expression Profile of Inflammatory Cytokines and Chemokines

Once the mice grew for their respective lengths and were sacrificed, qRT-PCR was performed to determine whether or not there was a difference in inflammatory mediator gene expression between 5xFAD and WT counterparts from 2- to 4-months. The mRNA fold changes for 5xFAD mice were compared to a fold change of 1 of WT counterparts for all genes of interest, which is indicated by the dotted line in Figure 2.

In 2-month 5xFAD males, TNF- α was significantly downregulated by 55% ($P < 0.05$; 2-way ANOVA; 95% CI: (0.176, 1.16); Figure 2 and Table 1b). Similarly, 5xFAD females showed a 48% reduction in the expression of TNF- α at this time period compared to WT counterparts ($P < 0.01$; 2-way ANOVA; 95% CI: (0.232, 1.17); Figure 2 and Table 1b).

In addition to TNF- α , IL-1 β was also significantly downregulated in 2-month 5xFAD males by 60% ($P < 0.01$; 2-way ANOVA; 95% CI: (0.209, 0.780); Figure 2 and Table 1b). Moreover, the mRNA fold changes for all inflammatory cytokines and chemokines of interest increased from the 2- to 3-month time-point in males. However, the differences in gene expression between WT and 5xFAD males at 3-months of age were not significant ($P > 0.05$; 2-way ANOVA; Figure 2 and Table 2b). In 4-month 5xFAD males, the only cytokine that showed a significant difference in gene expression was IL-6, which was downregulated by 55% compared to WT males ($P < 0.01$; 2-way ANOVA; 95% CI: (0.105, 1.95); Figure 2 and Table 3b).

In 5xFAD females, the only inflammatory chemokine that was significantly different at both 3- and 4-months was CXCL10. At 3-months, this gene had a 3.22-fold increase in gene expression compared to wild types ($P < 0.001$; 2-way ANOVA; 95% CI:

(1.36, 7.60); Figures 2 – 3 and Table 2b). CXCL10 also showed a robust gene expression at 4-months of age, with an mRNA fold change of 3.50 ($P < 0.01$; 2-way ANOVA; 95% CI: (0.489, 25.1); Figures 2 – 3 and Table 3b).

Gliosis

Along with examining the gene expression of various pro-inflammatory cytokines and chemokines, GFAP and IBA1 were chosen to detect any changes in gliosis, since astrocytes and microglia play a strong role in the immune response and are activated in response to CNS damage in neurodegenerative diseases.

In 5xFAD females, GFAP was continuously increasing over time and was significantly upregulated at both 3- and 4-months of age. At 3-months, GFAP had a 2.55-fold increase in gene expression compared to wild types ($P < 0.001$; 2-way ANOVA; 95% CI: (1.68, 3.88); Figures 2 – 3 and Table 2b). Similar to the pattern seen with CXCL10, GFAP also had a more pronounced increase in expression at 4-months with an mRNA fold change of 4.02 ($P < 0.01$; 2-way ANOVA; 95% CI: (0.936, 17.2); Figures 2 – 3 and Table 3b).

Upregulation of COX-2

In 5xFAD males, COX-2 was the only gene that was significantly upregulated at 4-months with an mRNA fold change of 2.00 ($P < 0.05$; 2-way ANOVA; 95% CI: (0.739, 5.40); Figures 2 and 4 and Table 3b). While the gene expression of COX-2 in 5xFAD females at 4-months of age was not significantly different compared to WT females, there is a general increase in expression from 2- to 3-months of age, which stabilizes at 4-months (Figures 2 and 4). Therefore, potentially growing female mice for 5-months

and beyond may show an induction of COX-2, similar to what was seen in the males (Figure 4).

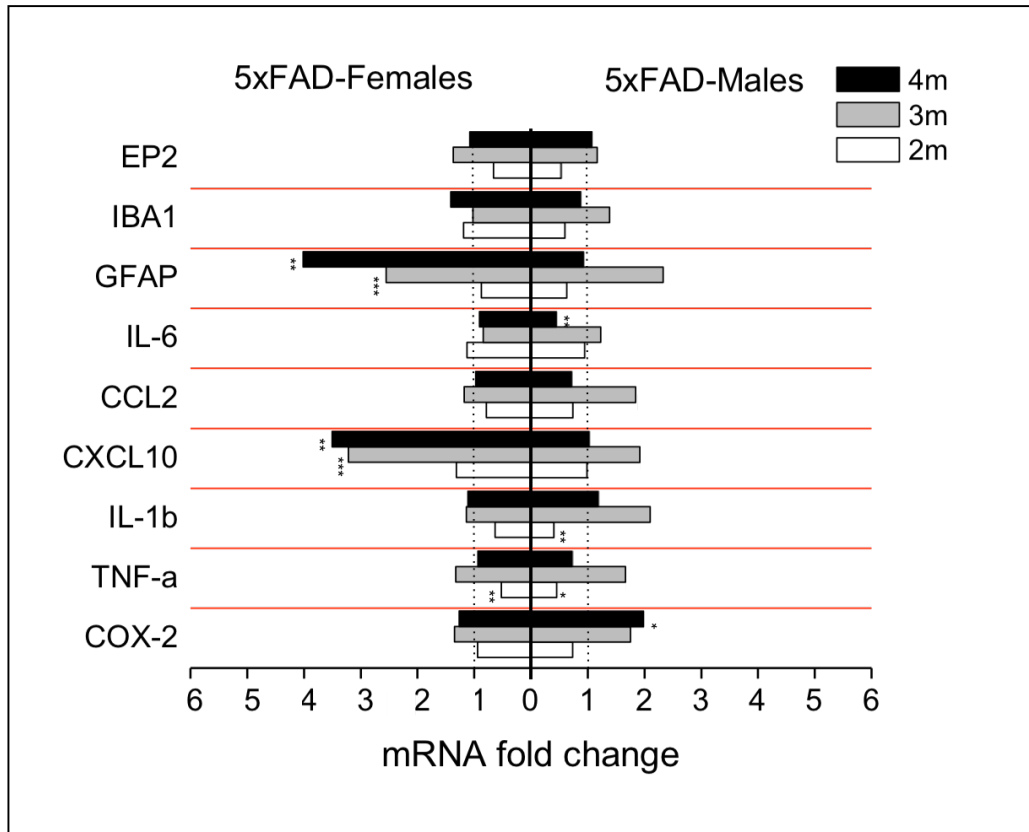


Figure 2. mRNA fold changes for 2-, 3-, and 4-month 5xFAD males and females for all genes of interest. Dotted line at 1 represents the mRNA fold change for all wild types. (* $P < 0.5$; ** $P < 0.01$; *** $P < 0.001$; 2-way ANOVA, Bonferroni post-hoc test).

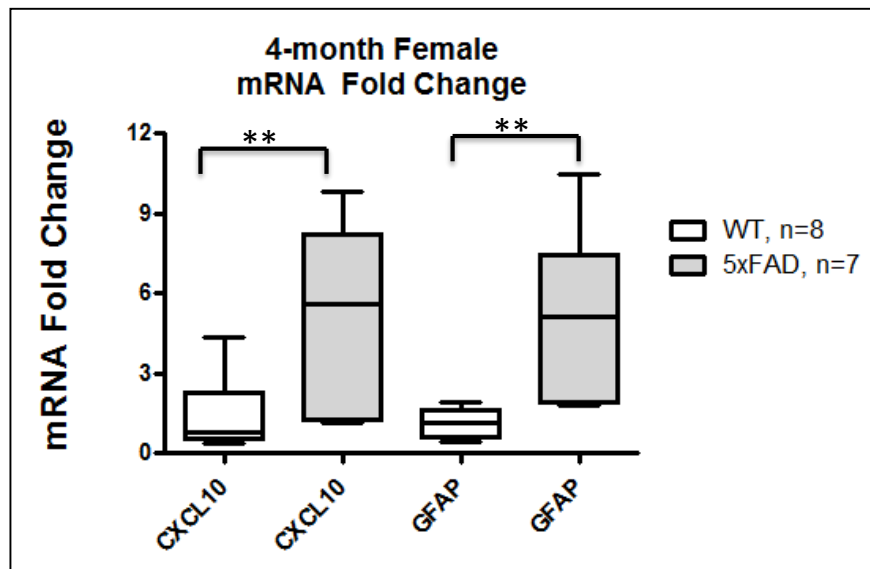


Figure 3. mRNA fold change for 4-month WT and 5xFAD females for CXCL10 and GFAP (** $P < 0.01$; 2-way ANOVA, Bonferroni post-hoc test using Δ CT values).

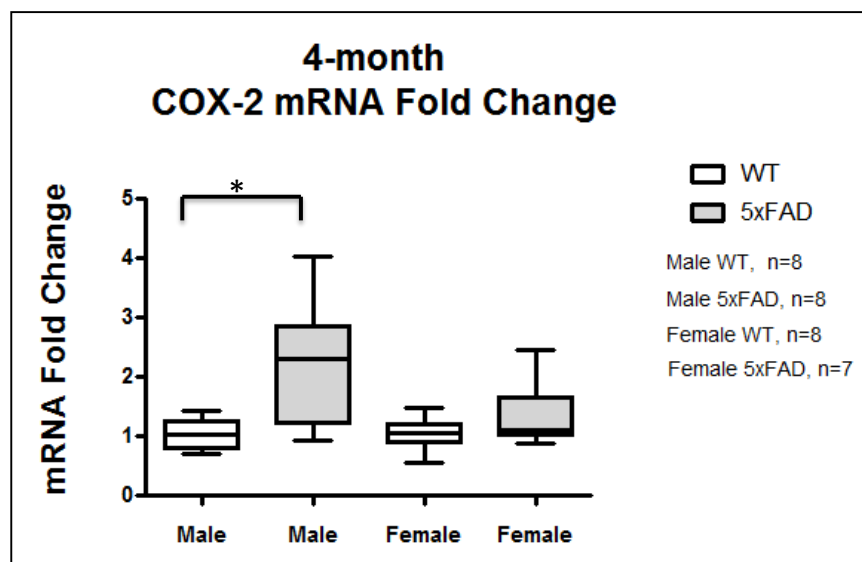


Figure 4. mRNA fold change for 4-month WT and 5xFAD males and females for COX-2 (* $P < 0.05$; 2-way ANOVA, Bonferroni post-hoc test using Δ CT values).

Congo Red Staining with IBA1

In addition to examining inflammatory gene expression, Congo red staining was performed to show the overall A β plaque pathology (in red) that developed in the cortex of a 4-month female WT and a 4-month female 5xFAD mouse. There is a greater accumulation of microglia (in black) in the 5xFAD female compared to the WT female (Figure 5). The staining illustrates how microglia are surrounding A β plaques in the 5xFAD female compared to being uniformly clustered in the WT female.

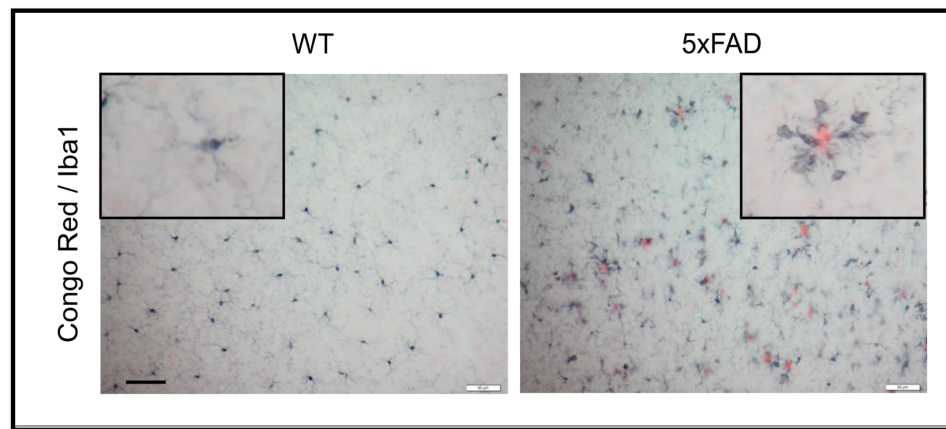


Figure 5. Congo Red Staining using IBA1 primary antibody spanning the cortex in a 4-month WT and a 4-month 5xFAD female mouse. Black indicates microglia and red indicates A β plaques. Scale bar represents 50 μ m; 40-micron thick sections were made using a freezing microtome.

Discussion

In a 5xFAD mouse model of AD, it was found that not all inflammatory mediators exhibited a continual increase in gene expression over time. The genes that were upregulated from 2- to 4-months in males (COX-2) did not parallel to those upregulated in females (CXCL10 and GFAP). A majority of the genes showed an increased expression from 2- to 3-months, yet this effect decreased at 4-months of age in males. Females showed a similar increase in gene expression from 2- to 3-months, yet the majority of the genes that were not significantly different remained at the same level from 3- to 4-months. This shows that studying inflammation over time is challenging because the levels of cytokines and chemokines in addition to glial cell markers and receptors such as EP2, which have been implicated in neuroinflammation, are constantly changing. Moreover, while previous studies have shown that inflammatory mediators play a detrimental role in AD, other studies have illustrated that they may be beneficial (Birch, Katsouri, and Sastre, 2014). For instance, microgliosis has been shown to either promote or protect the progression of AD pathology. Giulian et al. (1996) discovered that when microglia were incubated with neurons *in vitro*, this led to significant neuronal damage, and when microglia were not included in the culture, A β alone did not have any significant effects on neuronal survival. Contrastingly, Simard et al. (2006) demonstrated that bone marrow-derived microglia restricted plaque formation by promoting phagocytosis and A β clearance. There has also been a vast degree of controversy as to which specific inflammatory cytokines are upregulated or downregulated in AD, specifically those that have been more widely studied such as TNF- α and IL-6 (Brosseron et al., 2014). For instance, Uslu et al. (2012) found that low

serum A β -42 levels, which may be a possible biomarker for AD, were significantly associated with Mini-Mental State Examination scores of AD patients, yet there was no association with TNF- α or IL-6. Therefore, the roles of these mediators involved in the inflammatory process are not clearly understood, and further research needs to be conducted in order to elucidate how they may be correlated to the progression of AD.

In terms of the current study, it would be interesting to further examine the potential mechanisms driving the increase in inflammatory gene expression from 2- to 3-months, yet the decrease in gene expression at 4-months, a time when the 5xFAD mice exhibit apparent plaque deposition. Also, while microglia are considered to be the main resident immune cells in the brain, examining astrocyte expression may be helpful to better understand their role in AD, specifically since 5xFAD females showed an mRNA fold change of 2.55 and 4.02 at 3- and 4-months, respectively, compared to WT females (Bélanger and Magistretti, 2009).

Recently, there has been an increased focus on chemokines as inflammatory mediators in the CNS, and there is growing research to illustrate their role in the AD brain (Streit, Conde, and Harrison, 2001). One of the chemokines that has been associated with AD is CXCL10, which in the current experiment, showed robust mRNA expression at 3- and 4-months in 5xFAD females. Previous studies have shown that the upregulation of CCL4, also known as MIP-1 β , paralleled with an elevation of CXCL10 in reactive astrocytes of AD (Streit, Conde, and Harrison, 2001). Also, as A β accumulation results in aberrant neuronal activity, synaptic depression, and gliosis, there is a concurrent induction of CXCL10 more so by astrocytes and to a lesser degree by microglia (Xia et al., 2000; Palop and Mucke, 2010; Saruhan-Direskeneli et al.,

2003). This may be a possible explanation as to why the mRNA fold changes for both CXCL10 and GFAP observed in this study increased from 2- to 4-months in 5xFAD females. CXCL10 has been shown to increase levels of intracellular Ca^{2+} , which can activate caspase-3 and induce apoptosis (Sui et al., 2006). $A\beta$ has also been shown to increase intracellular Ca^{2+} levels *in vitro*, leading to neuronal death (Eimer and Vasser, 2013). Interestingly, previous *in vivo* studies have demonstrated that the 5xFAD mouse model exhibits increased levels of caspase-3 activation, so examining its gene expression in a time-dependent manner may be fruitful for future studies to develop a more comprehensive understanding of AD pathology (Eimer and Vasser, 2013).

Similar to the role of CXCL10 and the CXCR3 receptor, COX-2 can also mobilize Ca^{2+} by activating prostanoid receptors, thereby contributing to inflammation, pain, and neuronal injury in neurological diseases (Jiang and Dingledine, 2013; Figure 7). In the current study, COX-2 was the only gene in 5xFAD males that was continually upregulated over time and significantly differed at 4-months of age. Hoozemans et al. (2005) describe that the highest levels of neuronal COX-2 are observed in the first stages of AD pathology (Braak stages 0 – II, Braak A). Additionally, there is no significant difference in COX-2 immunoreactivity between Braak stage 0 and later Braak stages for neurofibrillary changes or $A\beta$ plaque deposition (Hoozemans et al., 2005). Moreover, the mean number of COX-2 immunoreactive neurons significantly decreases in Braak stages V and VI compared to in stage A for amyloid deposits (Hoozemans et al., 2005). These findings may provide a possible explanation for the results obtained in the current study. While COX-2 was significantly induced at 4-months in 5xFAD males, it is still an early time-point in this mouse model. Therefore, a future experiment could

take additional groups of 5xFAD and WT mice, allow them to grow them for a much longer period of time, for example, 9-months, in which this model exhibits neuronal loss, and determine at what time-point does the gene expression of COX-2 increase, remain unchanged, or begin to decrease. In a further study, it would be interesting to see whether COX-2 is downregulated at later months as indicated in Braak stages V and VI, and whether this same effect is evidenced in 5xFAD females as well.

In the current study, TNF- α was significantly downregulated in 5xFAD females at 2-months of age. In 5xFAD males, TNF- α and IL-1 β (at 2-months of age) and IL-6 (at 4-months of age) were all significantly downregulated. A possible reason for these results is that 2 – 4 months may not be a long enough time period to evidence a strong upregulation in these specific pro-inflammatory cytokines relative to WT counterparts. According to Bagyinszky et al. (2014), the expression of inflammatory cytokines such as IL-1 β , TNF- α , IL-6 is normally downregulated, and homeostasis is maintained by the counter-regulatory effects of anti-inflammatory cytokine such as IL-10, IL-4, and IL-13. However, it has been shown that the overproduction of pro-inflammatory cytokines over time may be involved in the progression of dementia and cellular damage (Lee, 2013; Szelényi, 2001). In the 5xFAD mouse model, Hillman et al. (2012) found that at 6-months of age, IL-1 β , TNF- α , and IL-6 were significantly upregulated by 2-, 2.1-, and 3-fold, respectively ($P < 0.05$). These previous studies indicate that these mice may need to grow for a greater period of time to exhibit differences in gene expression compared to WT counterparts. The aged mice would not only be more likely to present with neuroinflammation and A β deposition, but also with neuronal and synaptic loss.

Future Directions

The main focus of this study was to determine the levels of inflammatory mediators in the 5xFAD mouse model of both males and females in a time-dependent manner. As one brain hemisphere was used for qRT-PCR, the next step would be to use the other hemisphere to perform histology and examine protein levels of COX-2. Staining for astrocytes and microglia would also be helpful in order to understand their expression over time in this mouse model. Also, the other hemisphere can be used to perform additional Congo red staining to examine the progression of plaque deposition from 2- to 4-months.

Previous studies have shown that in the 5xFAD mouse model, A β -42 levels begin to rise as early as 1.5 months in females and plaque deposition begins at 2-months of age (Oakley et al., 2006). Therefore, an interesting question to examine for future studies is whether or not inflammation acts as a trigger or a consequence of AD. To answer this question, inflammatory gene expression of 5xFAD mice would need to be determined at 1-month of age compared to age-matched WT controls. If a significant difference is detected, this may suggest that inflammation is playing a role in the onset of plaque development.

The current treatment for AD includes the use of non-steroidal anti-inflammatory drugs (NSAIDs), which have been associated with delaying the onset of AD, slowing cognitive decline, and decreasing disease incidence by 25% – 80% (Szekely and Zandi, 2010). However, previous neuropathological analyses of post-mortem brain tissue have actually illustrated that NSAIDs reduced microglia activation rather than the amount of extracellular A β plaques (Hillmann et al., 2012). This most likely implies that NSAID use

in humans is suppressing neuroinflammation rather than inhibiting the pathological hallmarks of AD (Mackenzie and Munoz, 1998). Hillmann et al. (2012) found that chronic ibuprofen treatment to 5xFAD mice for 3 months led to an unchanged A β plaque load, an increase in soluble A β -42 levels, and an aggravation in behavior with the balance beam performance and the cross-maze alternation tests, exacerbating working memory. These previous studies most likely suggest that NSAIDs are not entirely effective at mitigating AD pathology.

Since NSAIDs work by inhibiting COX-1 and COX-2, which are upstream in the COX-2 signaling pathway, their site of action is not very specific. The Dingleline lab has developed a selective EP2 antagonist, TG6-10-1, as a more downstream target of neuroinflammation. According to Jiang et al. (2013), systemic administration of TG6-10-1 in a mouse pilocarpine model of status epilepticus reduced delayed mortality, accelerated recovery from weight loss, lowered brain inflammation, and offered neuroprotection in the hippocampus. In addition to status epilepticus, modulation of prostanoid receptors with an EP2 antagonist compared to NSAIDs may be effective in slowing cognitive decline in AD where inflammation is highly prevalent and a possible causal mechanism. In a future study, administering TG6-10-1 to 5xFAD mice that are 1-month of age may act as an early therapeutic strategy to mitigate neurodegeneration before A β -42 levels increase and plaques begin to develop.

As mentioned earlier, letting the 5xFAD mice grow for a longer period of time, such as 9-months when neuronal loss occurs, may be more helpful in seeing a greater induction of inflammation. Behavioral testing may also be performed to study spatial memory deficits, which begin at approximately 4 – 5 months of age based on the

phenotypic timeline in this model. Lastly, it would be interesting to assess long-term potentiation in the hippocampus, which becomes impaired at 6-months of age, to better discern memory loss in the 5xFAD mouse model.

Conclusion

This study shows that the gene expression of critical inflammatory mediators such as COX-2 in 5xFAD males and CXCL10 and GFAP in 5xFAD females has a time-dependent relationship, providing support for the hypothesis. However, other genes of interest do not show an overt increase in gene expression from 2 to 4-months, suggesting that the 5xFAD mouse model needs to be able to grow for a longer period of time as this time window is still representative of the early stages of AD.

AD is also an economic issue where the number of people that are diagnosed with the disease increases each year, which in turn, will lead to added healthcare spending. For example, it has been estimated that 24 million people worldwide are affected by dementia where the majority of these people have AD. If the disease continues at this rate, it is predicted that approximately 81 million people will be diagnosed by 2040 (Piaceri, Nacmias, and Sorbi, 2012). In addition to patient and family suffering, this disease is estimated to cost America alone \$1200 billion by 2050 (Alzheimer's Association, 2013). Treatment is both a national and a global issue, mainly since NSAIDs have not been efficacious in affecting the onset of AD pathology. Further research needs to be performed on more downstream targets where treatment can be administered to possibly mitigate the cognitive decline associated with AD.

Inflammation has been linked to most, if not all disease, specifically neurological and neurodegenerative diseases such as Alzheimer's. Therefore, this study can be

helpful in determining the early time course of inflammatory gene expression using the 5xFAD mouse model before giving any treatment. This may enable future experiments to better understand a possible mechanism by which these critical inflammatory mediators exert their effects and how they may be related to AD progression and pathology. Fundamentally, using this information from the basic science level *in vivo* may be beneficial in order to detect the earliest differences in inflammatory gene expression, which can hopefully be translated to the clinical level of AD in the future.

Limitations

One of the limitations of this study is that the 5xFAD mouse model does not develop neurofibrillary tangles. Therefore, this model may not completely mirror the pathology of AD in humans. However, it is still a useful model for research because it houses human FAD mutations, and it develops A β plaques as early as 2-months whereas other transgenic mouse models such as Tg2576 have to grow for at least 11 – 13 months to exhibit plaque deposition. Another potential weakness was that the sample size for 3-month male and female WT counterparts was slightly lower, which may have increased the variability in the results at this specific time-point. Lastly, using a half-brain for RNA extraction could have diluted the actual mRNA fold changes of the genes of interest. Future studies examining inflammatory gene expression at 1-month or later than 4-months of age could aim to only use the cortex or the hippocampus, since these are the brain regions where AD pathology is the most prominent.

References

- Alzheimer's Association. (2013). *Alzheimer's Disease Facts and Figures*. Chicago, IL: Alzheimer's Association. Available at: http://www.alz.org/alzheimers_disease_facts_and_figures.asp
- Bagyinszky, E., Youn, Y. C., An, S. S. A., & Kim, S. (2014). Characterization of inflammatory biomarkers and candidates for diagnosis of Alzheimer's disease. *BioChip Journal*. 8(3): 155-162.
- Bekris, L. M., Yu, C. E., Bird, T. D., & Tsuang, D. W. (2010). Genetics of Alzheimer Disease. *Journal of Geriatric Psychiatry and Neurology*. 23(4): 213–227.
- Bélanger, M., & Magistretti, P. J. (2009). The role of astroglia in neuroprotection. *Dialogues in clinical neuroscience*. 11(3): 281.
- Birch, A. M., Katsouri, L., & Sastre, M. (2014). Modulation of inflammation in transgenic models of Alzheimer's disease. *J Neuroinflammation*. 11: 25.
- Braak, H., Braak, E., Strothjohann, M. (1994). Abnormally phosphorylated tau protein related to the formation of neurofibrillary tangles and neuropil threads in the cerebral cortex of sheep and goat. *Neuroscience Letters*. 171(1-2): 1-4.
- Brosseron, F., Krauthausen, M., Kummer, M., & Heneka, M. T. (2014). Body fluid cytokine levels in mild cognitive impairment and Alzheimer's disease: a comparative overview. *Molecular neurobiology*. 50(2): 534-544.
- Chen, S. Y., Chen, T. F., Lai, L. C., Chen, J. H., Sun, Y., Wen, L. L., ... & Chen, Y. C. (2012). Sequence variants of interleukin 6 (IL-6) are significantly associated with a decreased risk of late-onset Alzheimer's disease. *J Neuroinflammation*. 24(9): 21-27.
- Cho, J., Nelson, T. E., Bajova, H., & Gruol, D. L. (2009). Chronic CXCL10 alters neuronal properties in rat hippocampal culture. *Journal of neuroimmunology*. 207(1): 92-100.
- Eimer, W. A., & Vassar, R. (2013). Neuron loss in the 5XFAD mouse model of Alzheimer's correlates with intraneuronal Abeta42 accumulation and Caspase-3 activation. *Mol Neurodegener*. 8(2).
- El Khoury, J., & Luster, A. D. (2008). Mechanisms of microglia accumulation in Alzheimer's disease: therapeutic implications. *Trends in pharmacological sciences*. 29(12): 626-632.

- El Khoury, J., Toft, M., Hickman, S. E., Means, T. K., Terada, K., Geula, C., & Luster, A. D. (2007). Ccr2 deficiency impairs microglial accumulation and accelerates progression of Alzheimer-like disease. *Nature medicine*. 13(4): 432-438.
- Gezen-Ak, D., Dursun, E., Hanağası, H., Bilgiç, B., Lohman, E., Araz, Ö. S., ... & Yilmazer, S. (2013). BDNF, TNF α , HSP90, CFH, and IL-10 serum levels in patients with early or late onset Alzheimer's disease or mild cognitive impairment. *Journal of Alzheimer's Disease*. 37(1): 185-195.
- Ghosh, S., Wu, M. D., Shafteel, S. S., Kyrkanides, S., LaFerla, F. M., Olschowka, J. A., & O'Banion, M. K. (2013). Sustained interleukin-1 β overexpression exacerbates tau pathology despite reduced amyloid burden in an Alzheimer's mouse model. *The Journal of Neuroscience*. 33(11): 5053-5064.
- Giulian, D., Haverkamp, L. J., Yu, J. H., Karshin, W., Tom, D., Li, J., ... & Roher, A. E. (1996). Specific domains of β -amyloid from Alzheimer plaque elicit neuron killing in human microglia. *The Journal of neuroscience*. 16(19): 6021-6037.
- Glass, C. K., Saijo, K., Winner, B., Marchetto, M. C., & Gage, F. H. (2010). Mechanisms underlying inflammation in neurodegeneration. *Cell*. 140(6): 918-934.
- Hartlage-Rübsamen, M., Zeitschel, U., Apelt, J., Gärtner, U., Franke, H., Stahl, T., ... & Rossner, S. (2003). Astrocytic expression of the Alzheimer's disease β -secretase (BACE1) is stimulus-dependent. *Glia*. 41(2): 169-179.
- Heneka, M. T., & O'Banion, M. K. (2007). Inflammatory processes in Alzheimer's disease. *Journal of neuroimmunology*. 184(1): 69-91.
- Hillmann, A., Hahn, S., Schilling, S., Hoffmann, T., Demuth, H. U., Bulic, B., ... & Wirths, O. (2012). No improvement after chronic ibuprofen treatment in the 5XFAD mouse model of Alzheimer's disease. *Neurobiology of aging*. 33(4): 833-e39.
- Hoozemans, J. J., Van Haastert, E. S., Veerhuis, R., Arendt, T., Scheper, W., Eikelenboom, P., & Rozemuller, A. J. (2005). Maximal COX-2 and ppRb expression in neurons occurs during early Braak stages prior to the maximal activation of astrocytes and microglia in Alzheimer's disease. *J Neuroinflammation*. 2: 27.
- Ishizuka, K., Kimura, T., Igata-yi, R. U. R. I. K. O., Katsuragi, S., Takamatsu, J., & Miyakawa, T. (1997). Identification of monocyte chemoattractant protein-1 in senile plaques and reactive microglia of Alzheimer's disease. *Psychiatry and clinical neurosciences*. 51(3): 135-138.

- Jiang, J., & Dingledine, R. (2013). Prostaglandin receptor EP2 in the crosshairs of anti-inflammation, anti-cancer, and neuroprotection. *Trends Pharmacol. Sci.* 34(7): 413-423.
- Jiang, J., Quan, Y., Ganesh, T., Pouliot, W., Dudek, F., Dingledine R. (2013). Inhibition of the prostaglandin receptor EP₂ following status epilepticus reduces delayed mortality and brain inflammation. (2013). *Proceedings of the National Academy of Sciences of the United States of America.* 110(9): 3591-3596.
- Krauthausen, M., Kummer, M. P., Zimmermann, J., Reyes-Irisarri, E., Terwel, D., Bulic, B., ... & Müller, M. (2015). CXCR3 promotes plaque formation and behavioral deficits in an Alzheimer's disease model. *The Journal of clinical investigation.* 125(1): 365-378.
- LaFerla, F. (2008). Amyloid- β and tau in Alzheimer's disease. *Nature Reviews Neuroscience.* May.
- Landel, V., Baranger, K., Virard, I., Lloriod, B., Khrestchatisky, M., Rivera, S., ... & Féron, F. (2014). Temporal gene profiling of the 5XFAD transgenic mouse model highlights the importance of microglial activation in Alzheimer's disease. *Molecular neurodegeneration.* 9(1): 33.
- Lee, M. (2013). Neurotransmitters and microglial-mediated neuroinflammation. *Current Protein and Peptide Science.* 14(1): 21-32.
- Lee, R. K., Knapp, S., Wurtman, R. J. (1999) Prostaglandin E₂ stimulates amyloid precursor protein gene expression: inhibition by immunosuppressants. *Journal of Neuroscience.* 19(3):940-947.
- Leissring, M. A., Farris, W., Chang, A. Y., Walsh, D. M., Wu, X., Sun, X., ... & Selkoe, D. J. (2003). Enhanced proteolysis of β -amyloid in APP transgenic mice prevents plaque formation, secondary pathology, and premature death. *Neuron.* 40(6): 1087-1093.
- Li, W., Poteet, E., Xie, L., Liu, R., Wen, Y., & Yang, S. H. (2011). Regulation of matrix metalloproteinase 2 by oligomeric amyloid β protein. *Brain research.* 1387: 141-148.
- Liang, X., Wang, Q., Hand, T., Wu, L., Breyer, R. M., Montine, T. J., & Andreasson, K. (2005). Deletion of the prostaglandin E₂ EP2 receptor reduces oxidative damage and amyloid burden in a model of Alzheimer's disease. *The Journal of neuroscience.* 25(44): 10180-10187.

- Liao, Y. F., Wang, B. J., Cheng, H. T., Kuo, L. H., & Wolfe, M. S. (2004). Tumor necrosis factor- α , interleukin-1 β , and interferon- γ stimulate γ -secretase-mediated cleavage of amyloid precursor protein through a JNK-dependent MAPK pathway. *Journal of Biological Chemistry*. 279(47): 49523-49532.
- Linke, R. P. (2006). Congo red staining of amyloid: improvements and practical guide for a more precise diagnosis of amyloid and the different amyloidoses. *Protein misfolding, aggregation, and conformational diseases*. 239-276.
- Liu, B., & Hong, J. S. (2003). Role of microglia in inflammation-mediated neurodegenerative diseases: mechanisms and strategies for therapeutic intervention. *Journal of Pharmacology and Experimental Therapeutics*. 304(1): 1-7.
- Mackenzie, I. R., & Munoz, D. G. (1998). Nonsteroidal anti-inflammatory drug use and Alzheimer-type pathology in aging. *Neurology*. 50(4): 986-990.
- Matousek, S. B., Ghosh, S., Shaftel, S. S., Kyrkanides, S., Olschowka, J. A., & O'Banion, M. K. (2012). Chronic IL-1 β -mediated neuroinflammation mitigates amyloid pathology in a mouse model of Alzheimer's disease without inducing overt neurodegeneration. *Journal of NeuroImmune Pharmacology*. 7(1): 156-164.
- Michlmayr, D., & McKimmie, C. S. (2014). Role of CXCL10 in central nervous system inflammation. *Int. J. Interferon Cytokine Mediator Res*. 6: 1-18.
- Montine, T. J., Sidell, K. R., Crews, B. C. (1999). Elevated CSF prostaglandin E₂ levels in patients with probable AD. *Neurology*. 53(7):1495-1498.
- Nelson, T. E., & Gruol, D. L. (2004). The chemokine CXCL10 modulates excitatory activity and intracellular calcium signaling in cultured hippocampal neurons. *Journal of neuroimmunology*. 156(1): 74-87.
- Oakley, H., Cole, S., Logan, S., Maus, E., Shao, P., Craft, J., et al. (2006). Intraneuronal β -amyloid aggregates, neurodegeneration, and neuron loss in transgenic mice with five familial alzheimer's disease mutations: potential factors in amyloid plaque formation. *The Journal of Neuroscience*. 26(40): 10129-10140.
- Palop, J. J., & Mucke, L. (2010). Amyloid-[beta]-induced neuronal dysfunction in Alzheimer's disease: from synapses toward neural networks. *Nature neuroscience*. 13(7): 812-818.
- Piaceri, I., Nacmias, B., & Sorbi, S. (2012). Genetics of familial and sporadic Alzheimer's disease. *Frontiers in bioscience (Elite edition)*. 5: 167-177.

- Pooler, A. M., Arjona, A. A., Lee, R. K., Wurtman, R. J. (2004) Prostaglandin E₂ regulates amyloid precursor protein expression via the EP2 receptor in cultured rat microglia. *Neuroscience Letters*. 362(2):127–130.
- Qi, H. P., Qu, Z. Y., Duan, S. R., Wei, S. Q., Wen, S. R., & Bi, S. (2012). IL-6-174 G/C and-572 C/G polymorphisms and risk of Alzheimer's disease. *PloS one*. 7(6): e37858.
- Querfurth, H. W., & LaFerla, F. M. (2010). Mechanisms of disease. *N Engl J Med*. 362(4): 329-344.
- Ricciotti E, FitzGerald G. (2011). Prostaglandins and inflammation. *Arteriosclerosis, Thrombosis, and Vascular Biology*. 31(5): 986–1000.
- Roßner, S., Lange-Dohna, C., Zeitschel, U., & Perez-Polo, J. R. (2005). Alzheimer's disease β -secretase BACE1 is not a neuron-specific enzyme. *Journal of neurochemistry*. 92(2): 226-234.
- Rodriguez, J. J., Witton, J., Olabarria, M., Noristani, H. N., & Verkhratsky, A. (2010). Increase in the density of resting microglia precedes neuritic plaque formation and microglial activation in a transgenic model of Alzheimer's disease. *Cell death & disease*. 1(1): e1.
- Rogers, J. T., Leiter, L. M., McPhee, J., Cahill, C. M., Zhan, S. S., Potter, H., & Nilsson, L. N. (1999). Translation of the Alzheimer amyloid precursor protein mRNA is up-regulated by interleukin-1 through 5'-untranslated region sequences. *Journal of Biological Chemistry*. 274(10): 6421-6431.
- Rubio-Perez J, Morillas-Ruiz J. (2012). A review: inflammatory process in Alzheimer's disease, role of cytokines. *The Scientific World Journal*. 756357.
- Saruhan-Direskeneli, G., Yentür, S. P., Akman-Demir, G., Işık, N., & Serdaroğlu, P. (2003). Cytokines and chemokines in neuro-Behçet's disease compared to multiple sclerosis and other neurological diseases. *Journal of neuroimmunology*. 145(1): 127-134.
- Scheffler, K., Stenzel, J., Krohn, M., Lange, C., Hofrichter, J., Schumacher, T., ... & Pahnke, J. (2011). Determination of spatial and temporal distribution of microglia by 230nm-high-resolution, high-throughput automated analysis reveals different amyloid plaque populations in an APP/PS1 mouse model of Alzheimer's disease. *Current Alzheimer research*. 8(7): 781.
- Sidoryk-Wegrzynowicz, M., Wegrzynowicz, M., Lee, E., Bowman, A. B., & Aschner, M. (2011). Role of astrocytes in brain function and disease. *Toxicologic pathology*. 39(1): 115-123.

- Simard, A. R., Soulet, D., Gowing, G., Julien, J. P., & Rivest, S. (2006). Bone marrow-derived microglia play a critical role in restricting senile plaque formation in Alzheimer's disease. *Neuron*. 49(4): 489-502.
- Sperling, R., & Johnson, K. (2010). Pro: Can biomarkers be gold standards in Alzheimer's disease? *Alzheimer's Research & Therapy*. 2(3): 17.
- Streit, W. J., Condeelis, J. R., & Harrison, J. K. (2001). Chemokines and Alzheimer's disease. *Neurobiology of aging*. 22(6): 909-913.
- Sui, Y., Stehno-Bittel, L., Li, S., Loganathan, R., Dhillon, N. K., Pinson, D., ... & Buch, S. (2006). CXCL10-induced cell death in neurons: role of calcium dysregulation. *European Journal of Neuroscience*. 23(4): 957-964.
- Szekely, C. A., & Zandi, P. P. (2010). Non-steroidal anti-inflammatory drugs and Alzheimer's disease: the epidemiological evidence. *CNS & Neurological Disorders-Drug Targets (Formerly Current Drug Targets-CNS & Neurological Disorders)*. 9(2): 132-139
- Szelényi, J. (2001). Cytokines and the central nervous system. *Brain research bulletin*. 54(4): 329-338.
- Takasugi, N., Tomita, T., Hayashi, I., Tsuruoka, M., Niimura, M., Takahashi, Y., ... & Iwatsubo, T. (2003). The role of presenilin cofactors in the γ -secretase complex. *Nature*. 422(6930): 438-441.
- Turner, P. R., O'Connor, K., Tate, W. P., & Abraham, W. C. (2003). Roles of amyloid precursor protein and its fragments in regulating neural activity, plasticity and memory. *Progress in neurobiology*. 70(1): 1-32.
- Uslu, S., Akarkarasu, Z. E., Ozbabalik, D., Ozkan, S., Çolak, O., Demirkan, E. S., ... & Alatas, O. (2012). Levels of amyloid Beta-42, interleukin-6 and tumor necrosis factor-alpha in Alzheimer's disease and vascular dementia. *Neurochemical research*. 37(7): 1554-1559.
- Viola, A., & Luster, A. D. (2008). Chemokines and their receptors: drug targets in immunity and inflammation. *Annu. Rev. Pharmacol. Toxicol.* 48: 171-197.
- Wilcock, D. M., Gordon, M. N., & Morgan, D. (2006). Quantification of cerebral amyloid angiopathy and parenchymal amyloid plaques with Congo red histochemical stain. *Nature protocols*. 1(3): 1591-1595.
- Xia, M. Q., Bacskai, B. J., Knowles, R. B., Qin, S. X., & Hyman, B. T. (2000). Expression of the chemokine receptor CXCR3 on neurons and the elevated expression of its ligand IP-10 in reactive astrocytes: in vitro ERK1/2 activation and role in Alzheimer's disease. *Journal of neuroimmunology*. 108(1): 227-235.

Zhang, F., & Jiang, L. (2015). Neuroinflammation in Alzheimer's disease. *Neuropsychiatric disease and treatment*. 11: 243-256.

Zhao, J., O'Connor, T., & Vassar, R. (2011). The contribution of activated astrocytes to Ab production: implications for Alzheimer's disease pathogenesis. *J Neuroinflamm*. 8: 150.

Supplementary Material

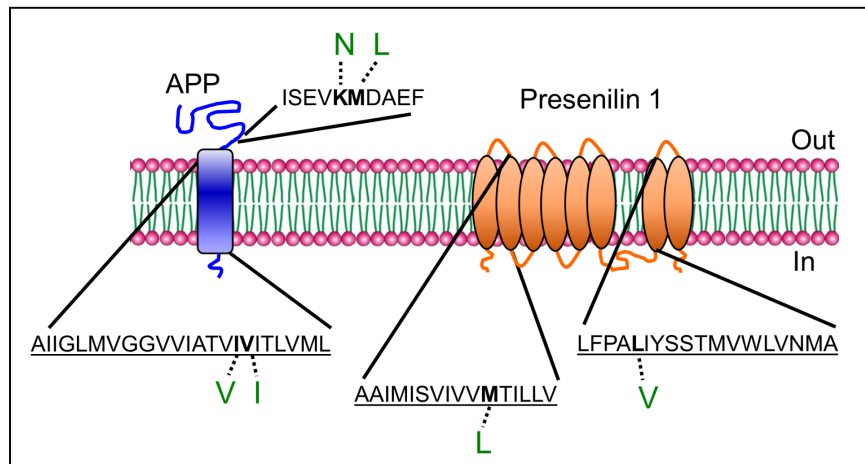


Figure 6. Human FAD mutations present on APP and PSEN1 in the 5xFAD mouse model. The Swedish double mutation on APP occurs when a lysine is mutated to an asparagine, and a methionine is mutated to a leucine at the base of the N-terminus. The Florida and London mutations occur within the transmembrane domain of APP where an isoleucine is mutated to a valine, and a valine is mutated to an isoleucine, respectively. The first PSEN1 mutation occurs in its second transmembrane domain where a methionine is mutated to a lysine. The second PSEN1 mutation, seen in the seventh transmembrane domain, occurs when a lysine is mutated to a valine.

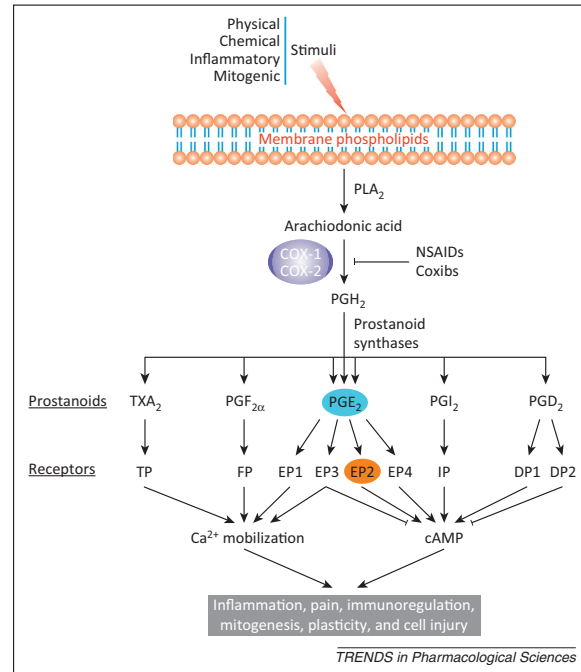


Figure 7. COX-2 Signaling Cascade. COX-2 activates prostanoid receptors, which play a role in inflammation, pain, and cell injury (Jiang and Dingledine, 2013).

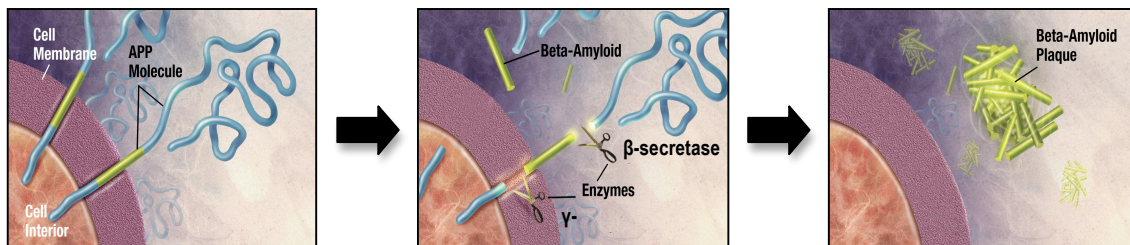


Figure 8. Generation of A β from APP. The enzyme that cleaves APP extracellularly is known as β -secretase 1 (BACE1), leaving a fragment that eventually gets degraded (in blue) and a soluble fragment that remains bound to the cell membrane (in green). A second enzyme, γ -secretase, cleaves this fragment, releasing the intracellular domain of APP and generating A β (Schenk et al., 1999).

Table 1a. Mean $\Delta\Delta\text{CT}$ values with standard deviations for 2-month WT and 5xFAD males and females.

Genes	WT Males (n = 6)		5xFAD Males (n = 8)		WT Females (n = 6)		5xFAD Females (n = 8)	
	Mean	SD	Mean	SD	Mean	SD	Mean	SD
COX-2	0.00	0.350	0.444	0.497	0.00	0.255	0.085	0.544
TNF- α	0.00	1.29	1.15	0.695	0.00	0.600	0.940	0.597
IL-1 β	0.00	0.485	1.31	0.484	0.00	0.454	0.656	0.417
CXCL10	0.00	0.746	0.028	0.714	0.00	0.413	-0.396	0.679
CCL2	0.00	0.561	0.433	0.538	0.00	0.286	0.344	0.232
IL-6	0.00	0.974	0.065	0.525	0.00	0.816	-0.175	0.531
GFAP	0.00	0.540	0.665	0.485	0.00	0.259	0.191	0.694
IBA1	0.00	0.683	0.747	0.445	0.00	0.203	-0.245	0.343
EP2	0.00	0.580	0.891	0.514	0.00	0.278	0.595	0.366

Table 1b. Mean mRNA fold changes with 95% Confidence Interval for 2-month WT and 5xFAD males and females.

Genes	WT Males (n = 6)		5xFAD Males (n = 8)		WT Females (n = 6)		5xFAD Females (n = 8)	
	Mean	95% CI	Mean	95% CI	Mean	95% CI	Mean	95% CI
COX-2	1.00	(0.622, 1.61)	0.735	(0.374, 1.44)	1.00	(0.707, 1.41)	0.943	(0.450, 1.97)
TNF- α	1.00	(0.172, 5.80)	0.452	(0.176, 1.16)	1.00	(0.442, 2.26)	0.521	(0.232, 1.17)
IL-1 β	1.00	(0.518, 1.93)	0.404	(0.209, 0.780)	1.00	(0.539, 1.85)	0.634	(0.360, 1.12)
CXCL10	1.00	(0.363, 2.76)	0.981	(0.372, 2.59)	1.00	(0.570, 1.75)	1.32	(0.523, 3.31)
CCL2	1.00	(0.467, 2.14)	0.741	(0.357, 1.54)	1.00	(0.678, 1.48)	0.788	(0.575, 1.08)
IL-6	1.00	(0.266, 3.76)	0.956	(0.468, 1.95)	1.00	(0.330, 3.03)	1.13	(0.549, 2.32)
GFAP	1.00	(0.480, 2.08)	0.631	(0.326, 1.22)	1.00	(0.704, 1.42)	0.876	(0.341, 2.25)
IBA1	1.00	(0.395, 2.53)	0.596	(0.326, 1.09)	1.00	(0.759, 1.32)	1.19	(0.744, 1.89)
EP2	1.00	(0.454, 2.20)	0.539	(0.268, 1.08)	1.00	(0.685, 1.46)	0.662	(0.403, 1.09)

Table 2a. Mean $\Delta\Delta\text{CT}$ values with standard deviations for 3-month WT and 5xFAD males and females.

Genes	WT Males (n = 4)		5xFAD Males (n = 6)		WT Females (n = 5)		5xFAD Females (n = 6)	
	Mean	SD	Mean	SD	Mean	SD	Mean	SD
COX-2	0.00	0.794	-0.819	0.704	0.00	0.224	-0.431	0.311
TNF- α	0.00	1.19	-0.722	0.813	0.00	0.555	-0.407	0.856
IL-1 β	0.00	1.63	-1.06	0.389	0.00	0.352	-0.185	0.940
CXCL10	0.00	1.38	-0.928	0.751	0.00	0.912	-1.69	0.632
CCL2	0.00	1.15	-0.896	0.883	0.00	0.130	-0.237	0.338
IL-6	0.00	1.07	-0.316	0.810	0.00	0.699	0.246	0.474
GFAP	0.00	0.894	-1.23	0.606	0.00	0.790	-1.35	0.308
IBA1	0.00	0.641	-0.452	0.398	0.00	0.249	-0.031	0.215
EP2	0.00	0.827	-0.225	0.599	0.00	0.767	-0.451	0.277

Table 2b. Mean mRNA fold changes with 95% Confidence Interval for 3-month WT and 5xFAD males and females.

Genes	WT Males (n = 4)		5xFAD Males (n = 6)		WT Females (n = 5)		5xFAD Females (n = 6)	
	Mean	95% CI	Mean	95% CI	Mean	95% CI	Mean	95% CI
COX-2	1.00	(0.340, 2.94)	1.76	(0.678, 4.59)	1.00	(0.738, 1.36)	1.35	(0.884, 2.06)
TNF- α	1.00	(0.199, 5.03)	1.65	(0.547, 4.98)	1.00	(0.471, 2.13)	1.33	(0.414, 4.24)
IL-1 β	1.00	(0.109, 9.15)	2.09	(1.23, 3.54)	1.00	(0.620, 1.61)	1.14	(0.317, 4.08)
CXCL10	1.00	(0.154, 6.49)	1.90	(0.686, 5.28)	1.00	(0.290, 3.45)	3.22	(1.36, 7.60)
CCL2	1.00	(0.210, 4.77)	1.86	(0.561, 6.17)	1.00	(0.838, 1.19)	1.18	(0.745, 1.87)
IL-6	1.00	(0.235, 4.26)	1.24	(0.414, 3.74)	1.00	(0.387, 2.58)	0.843	(0.443, 1.61)
GFAP	1.00	(0.297, 3.37)	2.34	(1.03, 5.33)	1.00	(0.342, 2.92)	2.55	(1.68, 3.88)
IBA1	1.00	(0.419, 2.39)	1.37	(0.797, 2.35)	1.00	(0.713, 1.40)	1.02	(0.763, 1.37)
EP2	1.00	(0.325, 3.08)	1.17	(0.518, 2.64)	1.00	(0.353, 2.84)	1.37	(0.938, 1.99)

Table 3a. Mean $\Delta\Delta\text{CT}$ values with standard deviations for 4-month WT and 5xFAD males and females.

Genes	WT Males (n = 8)		5xFAD Males (n = 8)		WT Females (n = 8)		5xFAD Females (n = 7)	
	Mean	SD	Mean	SD	Mean	SD	Mean	SD
COX-2	0.00	0.371	-0.998	0.732	0.00	0.428	-0.339	0.508
TNF- α	0.00	0.378	0.473	0.586	0.00	2.05	0.098	0.995
IL-1 β	0.00	0.446	-0.232	0.804	0.00	1.07	-0.149	0.921
CXCL10	0.00	0.489	-0.025	0.884	0.00	1.29	-1.81	1.45
CCL2	0.00	0.260	0.469	0.528	0.00	0.876	0.038	0.275
IL-6	0.00	0.399	1.14	1.08	0.00	1.06	0.136	0.271
GFAP	0.00	0.498	0.103	0.908	0.00	0.837	-2.01	1.07
IBA1	0.00	0.174	0.209	0.342	0.00	0.748	-0.501	0.371
EP2	0.00	0.406	-0.098	0.688	0.00	0.924	-0.109	0.377

Table 3b. Mean mRNA fold changes with 95% Confidence Interval for 4-month WT and 5xFAD males and females.

Genes	WT Males (n = 8)		5xFAD Males (n = 8)		WT Females (n = 8)		5xFAD Females (n = 7)	
	Mean	95% CI	Mean	95% CI	Mean	95% CI	Mean	95% CI
COX-2	1.00	(0.604, 1.66)	2.00	(0.739, 5.4)	1.00	(0.559, 1.79)	1.26	(0.634, 2.52)
TNF- α	1.00	(0.598, 1.67)	0.720	(0.325, 1.6)	1.00	(0.0616, 16.2)	0.93	(0.242, 3.61)
IL-1 β	1.00	(0.546, 1.83)	1.17	(0.394, 3.5)	1.00	(0.235, 4.25)	1.11	(0.317, 3.88)
CXCL10	1.00	(0.515, 1.94)	1.02	(0.306, 3.38)	1.000	(0.173, 5.77)	3.50	(0.489, 25.1)
CCL2	1.00	(0.703, 1.42)	0.723	(0.353, 1.48)	1.00	(0.304, 3.29)	0.97	(0.67, 1.41)
IL-6	1.00	(0.581, 1.72)	0.452	(0.105, 1.95)	1.000	(0.237, 4.21)	0.91	(0.629, 1.32)
GFAP	1.00	(0.508, 1.97)	0.931	(0.271, 3.2)	1.00	(0.321, 3.12)	4.02	(0.936, 17.2)
IBA1	1.00	(0.789, 1.27)	0.865	(0.543, 1.38)	1.00	(0.362, 2.76)	1.41	(0.854, 2.34)
EP2	1.00	(0.576, 1.74)	1.07	(0.42, 2.72)	1.00	(0.285, 3.51)	1.08	(0.646, 1.8)

Table 4a. *P*-values using Δ CT values of 2-, 3-, and 4-month males. (Ns denotes not significant; **P* < 0.5; ***P* < 0.01; ****P* < 0.001; 2-way ANOVA, Bonferroni post-hoc test).

Genes	P-values (Males)		
	2 Months	3 Months	4 Months
COX-2	ns	ns	*
TNF- α	*	ns	ns
IL-1 β	**	ns	ns
CXCL10	ns	ns	ns
CCL2	ns	ns	ns
IL-6	ns	ns	**
GFAP	ns	ns	ns
IBA1	ns	ns	ns
EP2	ns	ns	ns

Table 4b. *P*-values for Δ CT values of 2-, 3-, and 4-month females. (Ns denotes not significant; **P* < 0.5; ***P* < 0.01; ****P* < 0.001; 2-way ANOVA, Bonferroni post-hoc test).

Genes	P-values (Females)		
	2 Months	3 Months	4 Months
COX-2	ns	ns	ns
TNF- α	**	ns	ns
IL-1 β	ns	ns	ns
CXCL10	ns	***	**
CCL2	ns	ns	ns
IL-6	ns	ns	ns
GFAP	ns	***	**
IBA1	ns	ns	ns
EP2	ns	ns	ns

Table 5. Mean CT values for housekeeping gene, GAPDH, for 2-, 3-, and 4-month WT and 5xFAD males and females.

GAPDH	WT Males	5xFAD Males	WT Females	5xFAD Females
2-months	16.0 ± 0.1	15.8 ± 0.1	16.8 ± 0.1	16.7 ± 0.1
3-months	16.0 ± 0.3	16.0 ± 0.2	16.5 ± 0.1	16.6 ± 0.1
4-months	16.0 ± 0.1	16.1 ± 0.2	16.6 ± 0.1	16.3 ± 0.1

Table 6. Table of primers used for qRT-PCR. Each forward and reverse primer was 100 μM. When combined, each primer mix was 10 μM.

Genes	Forward Primer (sequence 5'-3')	Reverse Primer (sequence 5'-3')
β-ACTIN	CCAACCGTGAAAAGATGACC	CAATCAAGACGTTCTTTCCAGTT
GAPDH	TGTCCGTCGTGGATCTGAC	CCTGCTTCACCACCTTCTTG
HPRT1	GGTCCATTCTATGACTGTAGATTTT	CAATCAAGACGTTCTTTCCAGTT
COX-2	ACCAACGCTGCCACAAC	GGTTGGAACAGCAAGGATTT
TNF-α	TCTTCTGTCTACTGAACTTCGG	AAGATGATCTGAGTGTGAGGG
IL-1β	CAGGAAGGCAGTGTCACTCA	TCCCACGAGTCACAGAGGA
CXCL10	GTGCTGCTGAGTCTGAGTGG	TTGCAGGAATGATTTCAAGTTTT
CCL2	CATCCACGTGTTGGCTCA	GCTGCTGGTGATCCTCTTGTA
IL-6	AACTCCATCTGCCCTCAGGAACA	AAGGCAGTGGCTGTCAACAACATC
GFAP	GACAACTTTGCACAGGACCTC	ATACGCAGCCAGGTTGTTCT
IBA1	GGATTTGCAGGGAGGAAAAG	TGGGATCATCGAGGAATTG
EP2	TCTTTAGTCTGGCCACGATGCTCA	GCAGGGAACAGAAGAGCAAGGAGG

Table 7. Sample sizes for all 2-, 3-, and 4-month male and female WT and 5xFAD mice.

Type	n		
	2 Months	3 Months	4 Months
WT Male	6	4	8
5xFAD Male	8	6	8
WT Female	6	5	8
5xFAD Female	8	6	7